ChemPubSoc Europe

DOI: 10.1002/cctc.201601708

CHEMCATCHEM Communications

Single-Pot Conversion of Tetrahydrofurfuryl Alcohol into Tetrahydropyran over a Ni/HZSM-5 Catalyst under Aqueous-Phase Conditions

Elmira Soghrati,[a, b] Catherine Choong,[a] Chee Kok Poh,[a] Sibudjing Kawi,*[b] and Armando Borgna*[a]

Ni-based catalysts were examined in hydrogenolysis of tetrahydrofurfuryl alcohol, resulting in selective C–O bond breakage into 1,5-pentanediol, along with 1,2,5-pentanetriol, which was detected for the first time under aqueous-phase conditions. 70% yield to tetrahydropyran was achieved using one-pot conversion over a bifunctional Ni/HZSM-5 catalyst.

Biomass-derived furanic compounds, including furfural and 5-hydroxymethylfurfural (HMF), which can be derived through acid-catalyzed dehydration of pentoses and hexoses, are considered promising biorenewable platform chemicals.[1] Many studies have been carried out on upgrading them into a wide range of high value-added chemical intermediates and end products using heterogeneous catalysts.[2] For instance, total hydrogenation of furfural can produce tetrahydrofurfuryl alcohol (THFA) at a very high yield[3] from which various useful chemicals, such as 1,5-pentanediol (15PDO),[4] 3,4-2*H*-dihydropyran (DHP),[5] and 4-penten-1-ol,[6] can be obtained.

The first process for the synthesis of 15PDO starting from THFA is composed of three main steps, including dehydration of THFA to DHP, hydration of DHP to δ-hydroxyvaleraldehyde, followed by hydrogenation step to 15PDO, reaching on overall yield of around 70%.[5a] However, the disadvantage of such a process is the existence of several separation and purification steps in order to achieve this yield. Subsequently, recent experimental studies have been performed on direct conversion of furanics into pentanediols via a selective C–O bond hydrogenolysis reaction. It has been extensively reported that high activity and selectivity can be obtained over rhodium and iridium catalysts modified by oxophilic metals such as Re, Mo, and V oxides in the hydrogenolysis of THFA[4] and tetrahydropyran-2-methanol (2-THPM)[7] to their corresponding α,ω-diols (namely, 15PDO and 1,6-hexanediol). 15PDO can undergo a ring-closure pathway towards the formation of tetrahydropyran (THP) either in the presence of strong solid acid catalysts or high-temperature water (HTW).[8] Alternatively, THP can be produced via hydrogenation of DHP, which can be easily derived from dehydration of THFA.[9] THP can be used as a solvent, an intermediate in organic synthesis such as glutaric acid, 1,5-dichloropentane, heptanediamine, and pimelic acid.[9,10] There is not, however, any direct process using heterogeneous catalysts reported for the synthesis of THP, particularly starting from THFA.

The catalytic conversion of furanics over noble metal catalysts has been extensively studied in recent years. However, it is of great importance to develop catalytic systems based on non-noble metals due to the high cost and depleting resources of noble metals. Among non-noble metals, nickel-based catalysts are widely used in hydrogenation and hydrogenolysis reactions because of their good catalytic performance and low cost.[11] Huber et al. screened various alumina-supported monometallic catalysts including nickel, and found that only the Ni catalyst can produce 15PDO in aqueous-phase hydrogenolysis of THFA at temperatures above 523 K.[12] Resasco et al. also reported the C–O bond cleavage of tetrahydrofuran ring over Ni catalysts at temperatures higher than 473 K.[13] Therefore, the selective C–O cleavage of furanic-derived compounds over Ni catalysts is particularly encouraging and needs further investigations to understand the role of Ni as well as the mechanism of C–O bond cleavage over Ni particles. It is important to stress that depending on the catalyst, reactant, and process conditions, several reaction pathways can occur during C–O hydrogenolysis and various mechanisms can be proposed.

Herein, we first investigated the role of Ni metal sites using a Ni/SiO_2 catalyst along with the synergistic effect of both metal and acid sites on Ni/Al_2O_3 and Ni/HZSM-5 catalysts on the catalytic performances during the ring opening of cyclic ether compounds derived from furanic compounds, particularly THFA, under aqueous-phase conditions. Subsequently, we explored the reaction pathways as well as the respective reaction intermediates and products in THFA hydrogenolysis over Ni-based catalysts.

The catalytic activities of THFA hydrogenolysis over monometallic Ni catalysts and the respective support materials are reported in Table 1. The results over the Ni/SiO_2 catalyst (entry 1) show that Ni is capable of ring opening of THFA at the more sterically hindered secondary C–O bond, yielding mostly 15PDO with a selectivity of about 33% instead of 12PDO (7.5%). Regarding product distribution, two new reaction products, 1,2,5-pentanetriol (125PTO) and THP, are identified for the first time in the aqueous-phase hydrogenolysis of

[a] E. Soghrati, Dr. C. Choong, Dr. C. K. Poh, Dr. A. Borgna
Institute of Chemical and Engineering Sciences (ICES)
Agency for Science, Technology and Research (A*STAR)
1 Pesek Road, Jurong Island, Singapore 627833 (Singapore)
E-mail: Armando_Borgna@ices.a-star.edu.sg

[b] E. Soghrati, Prof. S. Kawi
Department of Chemical and Biomolecular Engineering
National University of Singapore
4 Engineering Drive 4, 117585 Singapore (Singapore)
E-mail: chekawis@nus.edu.sg

Supporting information for this article can be found under: http://dx.doi.org/10.1002/cctc.201601708.

Table 1. C–O bond hydrogenolysis of THFA over nickel-based catalysts.[a]

Entry	Catalyst	Catalyst/ reactant/ solvent [g/g/g]	THFA conversion [%]	Product selectivity [%] 15PDO	125PTO	12PDO	THP	2-HTHP	Others[a]	Rate [μmol gcat^{-1} min^{-1}]
1	Ni/SiO_2	0.3/3/57	7.9	33.1	11.1	7.5	6.7	0	20.3	33.5
2	Ni/Al_2O_3	0.3/3/57	6.1	14.7	13.4	9.8	4.9	0	29.4	25.5
3	Ni/HZSM-5	0.025/3/57	7.6	24.2	41.1	1.5	11.4	0.5	12.7	386.7
4	Ni/HZSM-5	0.05/3/57	17	36.6	17.7	0.8	19.2	0.3	9.6	431.6
5	Ni/HZSM-5	0.1/3/57	42.9	23.1	6.4	0	45.5	0.1	9.7	554.3
6	Ni/HZSM-5	0.2/3/57	89.5	5.9	0.3	0	60.9	0	6.8	560.9
7	Ni/HZSM-5	0.3/3/57	96.9	4	0.2	0	70.3	0	5.5	412.5
8	–	–/3/57	2.1	8.4	33.3	0	1.3	14.8	8.2	-
9	Ni/HZSM-5	0.05/60/–	9.5	5.9	0	2.1	23.2	0	8	4863.1
10	HZSM-5	0.1/3/57	28.9	27.4	11.8	0.4	10.1	7.3	10.2[b]	371.9

[a] Reaction conditions: 523 K, 34 bar H_2, 4 h, 5 wt% THFA in water (60 g). [a] Others include: 1-pentanol, 3-HTHP, 2-MTHF, THF, 1-butanol, and DVL. [b] Others plus DHP.

THFA. The product selectivity to 125PTO and THP over Ni/SiO_2 catalyst is approximately 11% and 7%, respectively. Various products including 1-pentanol, 3-hydroxytetrahydropyran (3-HTHP), 2-methyltetrahydrofuran (2-MTHF), tetrahydrofuran (THF), 1-butanol, and δ-valerolactone (DVL) are grouped together as "others" in Table 1. On the other hand, lower conversion, reaction rate, and selectivity to pentane polyols are achieved over Ni/Al_2O_3 (entry 2). This might be due to the formation of Ni aluminate species which are not easily reduced at the reduction temperature of 773 K (see the Supporting Information, Figure S1 and S3 for XRD and H_2-TPR data). Furthermore, considerable amount of THF and 1-butanol (21% combined selectivity of the products reported in others) are detected over Ni/Al_2O_3, being produced via first C–C hydrogenolysis of THFA side chain into THF, followed by C–O bond cleavage of THF into 1-butanol.[12] This clearly shows that Ni/Al_2O_3 catalyst is mostly active in the hydrogenolysis of CH_2OH side-chain group of THFA.

Interestingly, nickel supported on HZSM-5 zeolite is very active in the scission of C–O bond, attaining a combined selectivity of pentanediols and 125PTO of around 67%. 125PTO was the major product (with a selectivity of about 41%), followed by 15PDO (24%) using only few mg of Ni/HZSM-5 catalyst (entry 3 of Table 1). It is important to mention that a very small amount of Ni/HZSM-5 catalyst was used to achieve a similar conversion level, as compared to other supported Ni catalysts. We have further explored the catalytic performance of Ni/HZSM-5 catalyst at different conversion levels (entry 4–7) to have better insights into the product distribution during THFA hydrogenolysis. Employing increasing the catalyst amount, higher THFA conversion and higher yield of THP are obtained (see the Supporting Information, Figure S6 for more details). Interestingly, roughly complete THFA conversion after only 4 h is attained, resulting in the maximum THP yield of around 70% (entry 7). Compared to SiO_2- and Al_2O_3-supported Ni catalysts, considerably higher reaction rate (386.7 μmol gcat^{-1} min^{-1}) is observed on bifunctional Ni/HZSM-5 which is attributed to the presence of strong acidic sites on the bifunctional Ni/HZSM-5 catalyst (see the Supporting Information, Figure S4 for NH_3-TPD data). Additionally, both Brønsted and Lewis acid sites were observed on Ni/HZSM-5, whereas only Lewis acid sites are contributing in Ni/SiO_2 and Ni/Al_2O_3 catalysts (see the Supporting Information, Figure S5 for Pyr-IR data). In contrast, at high conversion levels, selectivity to 15PDO and 125PTO decreased substantially from 36.6% to 4% and 41.1% to 0.2%, respectively. Since 3-HTHP is one of the reaction products over Ni-based catalysts, we can conclude that 125PTO produced by THFA ring-opening, subsequently participates in dehydration pathway towards either 3-HTHP or starting material.[8] Furthermore, 15PDO can undergo the ring closure pathway, resulting in the formation of THP as a main product.[8] We should stress that this is the first time that THP is reported as a major product by one-pot hydrogenolysis of THFA using non-noble heterogeneous catalyst under aqueous-phase conditions.[5c,14] However, further investigation is needed to determine the dominating pathways in the direct production of THP over Ni/HZSM-5 catalyst.

As mentioned before, 125PTO is also detected as a reaction product over the all-monometallic nickel catalyst.■■ok?■■ It is notable that this is the first time that 125PTO is identified as a reaction product along with 15PDO in the hydrogenolysis of THFA. Previous studies over noble metals (Rh- or Ir-based catalysts) at 393 K did not report 125PTO as a reaction intermediate or byproduct from THFA.[4] Besides, another study of THFA hydrogenolysis at 523 K did not report 125PTO as one of reaction products over alumina-supported monometallic catalysts, particularly Ni.[12] However, Tomishige and co-workers reported the formation of 125PTO from furfuryl alcohol by ring-opening hydrolysis reaction and subsequent hydrogenation over rhenium-modified Rh–Ir alloy catalyst in one-pot conversion of furfural into 15PDO.[4h] Similarly, Dumesic et al. also identified 1,2,5,6-hexanetetrol, which originated from dihydroxymethylfuran via same reaction pathway.[15] However, these studies proposed the parallel acid-catalyzed hydrolysis and ring-opening routes, starting from unsaturated furan ring.

To have a better understanding regarding 125PTO production, we first examined THFA hydrogenolysis in a stainless-steel reactor in the absence of catalyst (entry 8). The results show that the C–O cyclic ether bond of THFA is cleaved in water at 523 K, forming 125PTO as major product with a selectivity of

33.3%, followed by 2-HTHP (14.8%) and 15PDO (8.4%). According to a previous report, water at near-critical region (523–623 K) has a strong tendency to ionize, and the hydronium ions produced by the dissociation of water can be involved in acid-catalyzed reactions.[16] Specifically, Lercher and co-workers have reported parallel hydrogenolysis and hydrolysis pathways in C–O bond hydrogenolysis of Lignin-derived compounds in the presence of water at 523 K.[11c,17] Moreover, the effect of water in the formation of 125PTO under the solvent-free (that is, water-free) reaction conditions was further investigated over Ni/ HZSM-5 catalyst (entry 9). Although the catalyst to reactant ratio was very low in the case of solvent-free reaction condition, nearly comparable conversion level (9.5%) as the reaction starting from 5 wt% THFA with the same catalyst amount (entry 4, 17%) is obtained. An extremely high reaction rate is achieved for the solvent-free reaction, suggesting that water has an inhibiting effect on the rate of THFA ring-opening reaction. Importantly, no 125PTO was detected in the absence of water, which proves that the third hydroxy group in the pentanetriol compound is provided by water under aqueous-phase reaction condition. However, it is fair to mention that some of the reaction products obtained in the run using pure THFA have not been identified.

We therefore propose that at high temperature and in the presence of small amounts of hydronium ions, ring-opening of tetrahydrofuran ring can occurred via a protonation step, followed by a S_N2 type reaction with water as a nucleophile (Scheme 1). As depicted in Scheme 1, the ring-opening is accompanied by deprotonation from water to generate the alcohol OH group. The bond cleavage through S_N2 type mechanism usually occurs at the sterically unhindered carbon center. In other words, the water molecule probably attacks the primary carbon, which is a less crowded site, and dissociates the bond to form primary carbocation intermediate. Another possibility is that S_N2 attack can take place at the sterically hindered side by CH_2OH substituent. Importantly, the product selectivity strongly depends on the stability of the cation intermediate formed in the different pathways. The carbocation intermediate formed via the later bond breakage can result in a more stable secondary carbocation intermediate. Currently, energy barriers derived from DFT are being calculated to unravel the most favorable route in 125PTO formation.

The impact of Ni was subsequently investigated by comparing the performance of bare HZSM-5 in the conversion of THFA under aqueous-phase conditions (entry 10). Comparing with the blank experiment, upon addition of HZSM-5, THFA conversion is significantly enhanced from 2.1% to 28.9%, suggesting that higher concentration of hydronium ion can remarkably promote ring-opening of THFA. Furthermore, the selectivities towards 15PDO and 125PTO are analogous to those in THFA hydrogenolysis over Ni/HZSM-5. Meanwhile, significantly lower selectivity towards THP (ca. 10% at the conversion of ca. 30%) is obtained over HZSM-5 as compared to that achieved over Ni/HZSM-5 catalyst (ca. 45% at a conversion level of ca. 40%). Interestingly, after incorporating any metal supported on HZSM-5 support (that is, Ni and Co; see the Supporting Information, Table S2), the mass balance and sum of the products were remarkably improved (>85%), as compared to the bare HZSM-5 (ca. 60%). This result shows the positive impact of hydrogenation site in the vicinity of zeolite acid sites on the reaction mechanism, inhibiting the side reaction in the formation of condensation products. Based on NH_3-TPD and Py-IR results (see the Supporting Information, Figures S4 and S5 and Table S1), after incorporation of Ni, the concentration of Brønsted acid sites decreases significantly due to the ion exchange of Brønsted acid sites with Ni^{2+}, while the concentration of Lewis acid sites increases. This is attributed to the creation of the stronger acidic groups between NiO and HZSM-5, resulting a strong desorption peak in the NH_3-TPD profile of Ni/HZSM-5, as compared with HZSM-5. However, according to a previous report,[18] after catalyst reduction, the Brønsted acid sites of Ni/HZSM-5 can be recovered (close to that of parent HZSM-5) owing to generation of Ni^0 particles from zeolite exchange sites. In contrast, the concentration of Lewis acid sites decreases significantly because of reduction of Ni^{2+}.

Interestingly, we also detect 2-HTHP (7.3%) and very small amount of DHP (1.7%) in THFA ring-opening over HZSM-5 zeolite. As mentioned before, the reaction pathway of the multistep conversion of THFA to 15PDO has been reported via DHP formation as a dehydration product of THFA in the first step over acidic catalyst (Al_2O_3).[5] Similarly, THFA dehydration into DHP can occur over HZSM-5, followed by further hydrolysis step into δ-hydroxyvaleraldehyde or 2-HTHP. In the meantime, since DHP is not very stable under the reaction conditions, it can be hydrogenated into THP over Ni catalyst.[19] Indeed, DHP is not detected over monometallic Ni-based catalyst, particularly Ni/HZSM-5. Importantly, as compared to Ni/HZSM-5, a considerably higher selectivity to 2-HTHP (7.3%) was obtained over HZSM-5 without Ni. Therefore, the pathway through DHP and 2-HTHP might contribute to the production of 15PDO and THP under aqueous-phase reaction conditions over Ni-based catalysts, particularly Ni/ HZSM-5 catalyst.

Since the bifunctional Ni/HZSM-5 catalyst was the most active Ni-based catalyst for aqueous-phase hydrogenolysis of

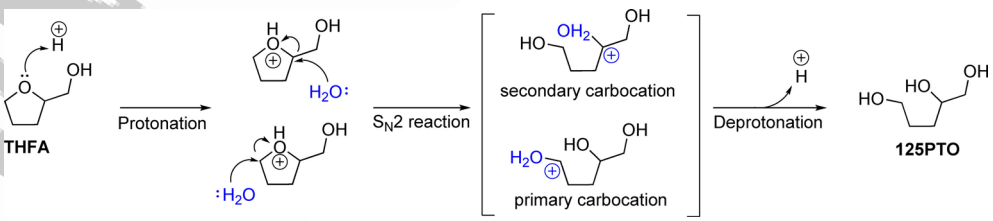

Scheme 1. Proposed reaction pathway of 1,2,5-pentanetriol production.

THFA at 523 K (with the highest reaction rate of around 560 μmol gcat^{-1} min^{-1}), this catalyst was further investigated. Figure 1 shows the evolution of the reaction products formed during THFA hydrogenolysis over Ni/HZSM-5 as a function of

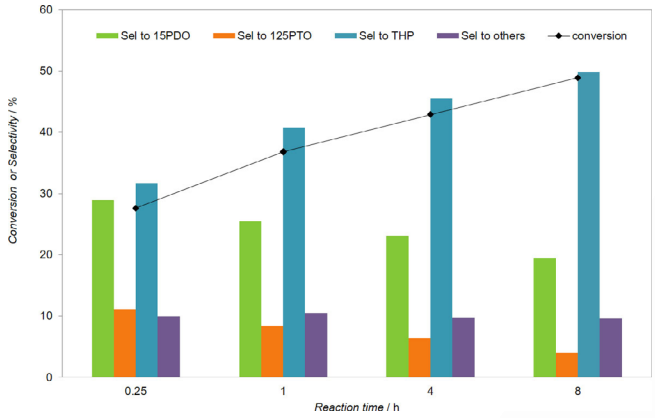

Figure 1. C–O bond hydrogenolysis of THFA over Ni/HZSM-5 at different reaction times. Reaction conditions: 523 K, 34 bar H_2, 0.1 g catalyst, 5 wt% THFA in water. Others include: 12PDO, 1-pentanol, 3-HTHP, 2-HTHP, 2-MTHF, THF, 1-butanol, and DVL.

the conversion level. The results show that 15PDO and 125PTO are initially produced over Ni/HZSM-5 catalyst via hydrogenolysis and hydrolysis pathways, respectively. Meanwhile, acid-catalyzed dehydration routes lead to the formation of THP, even at a very short reaction time (15 min). At longer reaction times, higher conversion and THP yield are gradually obtained, suggesting that both 125PTO and 15PDO are intermediate products in THP production. Moreover, Ni/HZSM-5 catalyst is not very active for over-hydrogenolysis of 15PDO to 1-pentanol since the selectivity toward 1-pentanol remained nearly constant as a function of the conversion level. We therefore conclude that ring-opening of THFA initially occurs over both nickel metal sites and HZSM-5 acidic sites, undergoing further dehydration and ring closure over acidic sites, yielding THP.

To better understand the reaction mechanism in the formation of THP, the hydrogenolysis reaction starting from reaction intermediates (125PTO, 15PDO, and DHP) were studied, and the results are reported in Table 2, 3, and 4, respectively. As shown in Table 2, 125PTO conversion can proceed in water in the absence of catalyst, forming THFA as a main product (that is, 55.8% selectivity). Similarly, it has been reported that cyclodehydration of polyols can proceed in the presence of high-temperature water.[8] In the case of 125PTO dehydration, higher yield of the five-membered cyclic ethers (that is, THFA) than the six-membered ones (that is, 3-HTHP) can be obtained.[8] The HZSM-5 support is on the one hand enhancing the formation THP, as compared with the reaction in the absence of catalyst. On the other hand, lower 125PTO conversion is observed, speculating that THFA, produced by dehydration of 125PTO over either HTW or HZSM-5, can further participate in hydrolysis pathway towards 125PTO formation. In contrast, upon addition of Ni/SiO_2 and Ni/HZSM-5 catalysts, the catalytic activity and THFA yield are considerably enhanced. Moreover,

Table 2. C–O bond hydrogenolysis of 125PTO over nickel-based catalysts.[a]

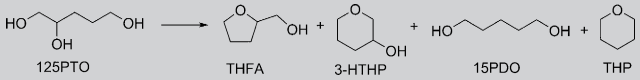

Catalyst	Reactant	Conversion [%]	Product selectivity [%]				
			THFA	3-HTHP	15PDO	THP	Others[b]
–	125PTO	32.8	55.8	3.1	5.6	3.2	4.4
HZSM-5		22.8	37	3.5	11.5	17.9	13.1[c]
Ni/SiO_2		62.6	41.9	2.5	5.9	2.3	8.2[d]
Ni/HZSM-5		>99.9	40.4	2.1	7.1	21.7	3.9

[a] Reaction conditions: 523 K, 34 bar H_2, 4 h, 1 wt% reactant in water, 10Ni/SiO_2 (0.3 g), 10Ni/HZSM-5 (0.1 g), [b] Others including: 1-pentanol, 2-MTHF, THF, and 1-butanol. [c] Others plus 2-HTHP. [d] Others plus 12PDO.

higher yields of THP and 15PDO are obtained over Ni/HZSM-5, suggesting that THFA produced through ring closure of 125PTO, can be subsequently participated in THP and 15PDO formations. Similarly, 15PDO can undergo the ring-closure pathway, resulting in the formation of THP as a main product (Table 3). The activity trend of 15PDO dehydration is compara-

Table 3. C–O bond hydrogenolysis of 15PDO over nickel-based catalysts.[a]

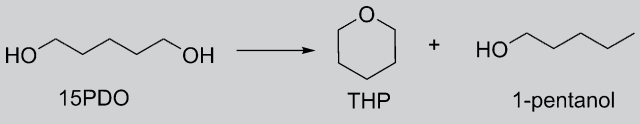

Catalyst	Reactant	Conversion [%]	Product selectivity [%]	
			THP	1-pentanol
–	15PDO	7.7	44.6	9.3
HZSM-5		97	81.3	0.2
Ni/SiO_2		14.5	54.8	7.7
Ni/HZSM-5		94.9	83.6	2

[a] Reaction conditions: 523 K, 34 bar H_2, 4 h, 1 wt% reactant in water, 10Ni/SiO_2 (0.3 g), 10Ni/HZSM-5 (0.1 g).

ble with that of 125PTO dehydration. Higher THP yield (around 80%) is achieved over HZSM-5 and bifunctional Ni/HZSM-5 catalyst, as compared with the reaction over Ni/SiO_2 and blank experiment. As described before concerning the hydrogenolysis of THFA, these results also suggest that ring-opening first occur to produce pentane polyols, followed by acid-catalyzed dehydration pathways to form THP.

To study further the route starting from dehydration pathway, the catalytic activity of DHP in hydrogenolysis reaction was also examined and the results are reported in Table 4. In all experiments, roughly complete conversion is obtained, suggesting that DHP is not very stable under reaction condition. In the absence of catalyst, 15PDO is formed as a main product with yield of 46.5%, followed by 2-HTHP (12.3%). According to a previous report,[5a] 2-HTHP can be formed as a hydrolysis product of DHP under very mild reaction conditions and in the presence of acid (HCl). Hydrogenolysis of DHP over HZSM-5

Table 4. C–O bond hydrogenolysis of DHP over nickel-based catalysts.[a]

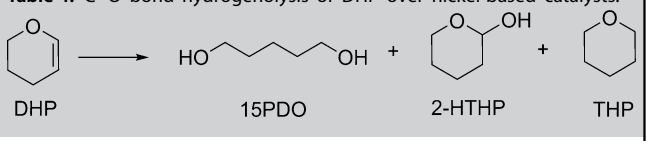

Catalyst	Reactant	Conversion [%]	Product selectivity [%]		
			15PDO	2-HTHP	THP
–	DHP	>99.9	46.5	12.3	3.8
HZSM-5		>99.9	32.4	9.2	2.0
Ni/SiO_2		>99.9	1.4	0	54.5
Ni/HZSM-5		>99.9	17.9	0	47
Ni/HZSM-5[b]		>99.9	36.3	0	29.5

[a] Reaction conditions: 523 K, 34 bar H_2, 4 h, 1 wt% reactant in water, 10Ni/SiO_2 (0.3 g), 10Ni/HZSM-5 (0.1 g) [b] 1 h reaction time.

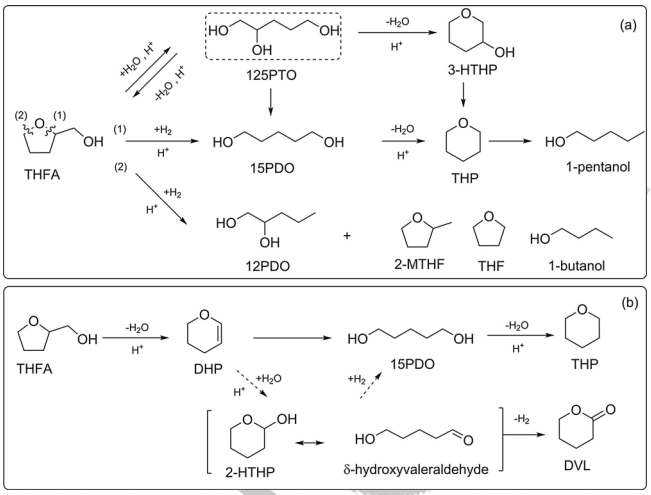

Scheme 2. Overall reaction pathway for the a) direct and b) indirect C–O hydrogenolysis of THFA under aqueous-phase conditions at 523 K.

also shows similar trend with poorer yields, which might be attributed to an enhancement on polymerization reactions over acid sites of HZSM-5.[5a] Over Ni/SiO_2 catalyst and in the absence of strong acid sites, THP is formed as a main product (with the yield of 54.5%), suggesting that Ni directly hydrogenates C=C double bond of DHP without participating in the ring-opening pathway. Furthermore, a combined yield of 15PDO and THP of around 65% is attained over Ni/HZSM-5 after 4 h. To further understand the ring-opening pathway over Ni/HZSM-5, the DHP hydrogenolysis reaction was examined at a shorter reaction time (1 h), indicating that DHP is completely converted after 1 h and the combined selectivity of 15PDO and THP is roughly similar to the one obtained at longer reaction time. These results suggest that DHP is rapidly participated in parallel hydrolysis and ring-opening reactions over Ni/HZSM-5 to 2-HTHP (that is, stable hemiacetal of δ-hydroxyvaleraldehyde), followed by formation of 15PDO from which THP can be formed through ring-closure pathway.

As discussed above, the catalytic hydrogenolysis of THFA in aqueous-phase is a complex process, including ring-opening of the cyclic ether bond, hydrogenation, dehydration, ring closure, and hydrolysis steps. Moreover, in this study we have investigated the role of different active sites involved in the reaction, including Ni metal sites, HZSM-5 acid sites, and the bifunctional acid-metal sites of Ni/HZSM-5 catalysts. Based on the experimental results, the overall reaction pathway of the conversion of THFA in aqueous-phase at high temperature (523 K) is proposed in Scheme 2. As shown in Scheme 2a, direct THFA hydrogenolysis can initially occur via different pathways, mainly involving cleavage of two cyclic C–O ether bonds, forming 15PDO and 12PDO. The C–O bond cleavage of the less sterically hindered side of THFA molecule into 12PDO is not favorable over Ni-based catalysts. Additionally, 125PTO as a new ring-opening product is formed by an acid-catalyzed hydrolysis pathway. Determining the energy barriers of the individual pathways can elucidate which breakage of C–O cyclic bond is favored over Ni catalysts in the presence of acid sites. 15PDO can further undergo dehydration over acid sites, resulting in the THP formation as the main product over Ni/HZSM-5 catalyst. Similarly, dehydration of 125PTO can lead to reverse reaction path into THFA as well as 3-HTHP product. Finally, over-hydrogenolysis of the resulting C_5 polyols can also take place, although it is not as favorable as the ring-closure pathway over Ni catalysts. Besides, the THFA hydrogenolysis is also accompanied with several side reactions, resulting in the formation of a small amount of 2-MTHF and THF. In the meantime, the indirect hydrogenolysis pathway, starting with a dehydration step (Scheme 2b), takes place to produce DHP and 2-HTHP as intermediates in the production of 15PDO and THP. DVL can also be formed via dehydrogenation of 2-HTHP, which was detected in small amounts over Ni catalysts.

The recycling performances of the representative Ni/HZSM-5 catalyst for THFA hydrogenolysis are shown in the Supporting Information, Figure S7. Compared with the fresh Ni/HZSM-5 catalyst, the THFA conversion decreased from around 97% to around 78% in the second run, and dropped to approximately 30% in the third recycle run. To understand the loss of activity during the three recycling runs, we investigated catalyst physical changes including Ni crystallite size between the fresh and used catalysts. The characterization of Ni particles by XRD method (calculated by fitting of Rietveld refinement of the XRD data; Supporting Information, Figure S2 and Table S1) provides the domain size of around 20 nm for the fresh Ni/HZSM-5 catalyst. However, the Ni crystallite size of spent catalyst determined by XRD method is much larger (around 50 nm), as compared to the fresh catalyst. This result shows a significant overgrowth of Ni crystallites size after hydrogenolysis reaction, resulting in rapid deactivation of Ni/HZSM-5 catalyst.[18] The crystallite size of HZSM-5 remained roughly constant at 50 nm, indicating the preservation of the zeolite structure in the spent Ni/HZSM-5 catalyst after hydrothermal condition.

Additionally, Ni and Al losses by leaching at hydrothermal condition were evaluated after three recycling runs (Supporting Information, Table S3). Compared to the original loading, Ni weight loss from Ni/HZSM-5 catalyst is around 4–5 wt% at different recycling runs, indicating weak interaction between Ni and HZSM-5 support. In contrast, Al leaching is almost negli-

gible under the present reaction condition. The presence of active soluble species in the reaction medium was investigated in THFA hydrogenolysis by using the liquid phase after contacting with Ni/HZSM-5 catalyst (without substrate) for 4 h at the same reaction condition.[20] The result showed that the leached species did not have any significant impact on activity of Ni/HZSM-5 catalyst.

In summary, in this study, we focused on understanding the reaction mechanism of THFA hydrogenolysis as well as identifying reaction intermediates and products over Ni-based catalysts in the presence of high-temperature water (523 K). The results over Ni metallic sites show that Ni efficiently promotes THFA hydrogenolysis at the more sterically hindered secondary C–O bond, yielding mostly 15PDO instead of 12PDO. Furthermore, THFA hydrogenolysis can proceed in parallel through protonation and S_N2-type reaction with water (solvent), yielding 1,2,5-pentanetriol as new reaction intermediate of THFA conversion under aqueous-phase condition. Moreover, ring-opening of THFA can occur over both nickel metallic sites and HZSM-5 acid sites, followed by ring closure to yield tetrahydropyran over acid sites in a single step, resulting in up to around 70% yield. Different reaction mechanisms such as direct and indirect pathways are contributing in the ring-opening of THFA to produce 15PDO and THP.

Experimental Section

Catalyst preparation

Silica (Kanto), alumina (Merck), and NH_4-ZSM-5 with a Si/Al ratio of 80 (Zeolyst) were used as support materials. The ammonium form of ZSM-5 was calcined in air at 773 K for 4 h prior to use. The supported nickel catalysts were prepared by incipient wetness impregnation method using an aqueous solution of nickel nitrate hexahydrate (Alfa Aesar). The Ni loading was 10 wt.%. After impregnation, the catalysts were dried (383 K), calcined in air (773 K), reduced in flowing H_2 (773 K), and then passivated with flowing 1%O_2 in N_2 (298 K) before exposing to air.

Catalyst characterizations

The Brunauer–Emmett–Teller (BET) surface areas of the catalysts were determined through nitrogen adsorption at 77 K using a Micromeritics ASAP-2020 adsorption apparatus. Prior to the measurements, the samples were degassed in vacuum at 473 K overnight.

The final loading of Ni was determined by X-ray Fluorescence (XRF) measurements using a spectrometer (S4 Explorer, Bruker AXS).

Powder X-ray diffraction (XRD) patterns were recorded on a Bruker D8 Advance diffractometer using filtered $Cu_{K\alpha}$ radiation ($\lambda =$ 1.5406 Å) produced by an X-ray source and operated at 35 kV and 40 mA. The diffraction patterns were taken in the Bragg angle (2θ) range from 20° to 80°. The XRD data were evaluated with the whole pattern fitting according to the Rietveld method (TOPAS software).

H_2-temperature-programed reduction (H_2-TPR) measurement for the fresh catalyst was performed on TPD/R/O 1100 system (Thermo Scientific) equipped with a thermal conductivity detector (TCD). Prior to TPR measurement, 50 mg of catalyst was outgassed in Ar at 473 K for 1 h to remove impurities and then cooled down to room temperature. 5% H_2/N_2 gas was passed through the catalyst bed (50 mL min^{-1}), while the temperature of the furnace was increased from 323 to 1173 K at a heating rate of 10 K min^{-1}.

NH_3-temperature programed desorption (NH_3-TPD) was also conducted on TPD/R/O 1100 instrument. About 100 mg of catalyst was loaded into the quartz tube, outgassed in Ar at 473 K for 1 h, and then cooled down to room temperature. The catalyst was exposed to NH_3 (50 mL min^{-1}) for 1 h, and subsequently the sample was flushed with He for 1 h to remove physisorbed molecules. For the TPD measurement, the catalyst was heated up in flowing He (50 mL min^{-1}) from 303 to 973 K with a temperature ramp rate of 10 K min^{-1} to desorb ammonia.

The IR spectra of chemisorbed pyridine (Pyr-IR) were recorded using a Fourier transform infrared spectrometer (BIO-RAD Excalibur series FTS 3000). The sample was prepared as a self-supporting wafer and outgassed in vacuum at 573 K for 1 h, and cooled to room temperature, followed by exposure of the sample to pyridine vapor. The IR spectra of chemisorbed pyridine were recorded subsequently in the spectral range of 400–4000 cm^{-1} at a resolution of 4 cm^{-1}. 128 scans were recorded for each spectrum. The desorption of pyridine was carried out through heating the wafer from room temperature to 373 K, 473 K and 573 K and held at each temperature for half an hour.

Catalytic measurements

All hydrogenolysis experiments of THFA were carried out in a 100 mL stainless-steel autoclave reactor (Parr instrument). For each reaction, THFA (5 wt%), water, and the appropriate amount of catalyst were loaded into the reactor. The reactor was sealed, purged three times with hydrogen, and then pressurized to 34 bar with H_2. The reactor was then heated to the required temperature, using a stirring rate of 500 rpm. Once the reaction time was completed, the reactor was cooled to room temperature. The liquid products were collected and transferred to vials and the catalyst was separated by centrifugation and filtration.

Analytical methods

Quantitative analysis of liquid products were performed using gas chromatograph (Agilent, 6890 N) equipped with a HP-1 and CP-Wax 57 CB columns and a flame ionization detector (FID). Identification of products was performed using a gas chromatograph–mass spectrometer (Agilent 6890 N, GC-MS) equipped with a HP-1MS capillary column, and matched to at least 95% similarity with purchased compounds, references from the NIST MS library, or previous reports. Additionally, liquid chromatography/ time-of-flight mass spectrometry (LC/TOF-MS) studies were also carried out by using reversed-phase Rezex ROA-Organic Acid H^+ (8%) column and Milli-Q water with formic acid■■ok?■■ as the organic modifier with the gradient program. Inductively coupled plasma atomic emission spectrometry (ICP-AES) was used to detect the presence of Ni and Al in reaction solutions.

Acknowledgements

*The authors gratefully acknowledge the Singapore Agency for Science, Technology and Research (A*STAR) for their financial supports.*

Conflict of interest

The authors declare no conflict of interest.

Keywords: hydrogenolysis · Ni/HZSM-5 · tetrahydrofurfuryl alcohol · tetrahydropyran

[1] J. J. Bozell, G. R. Petersen, *Green Chem.* **2010**, *12*, 539 – 554.
[2] a) Y. Nakagawa, K. Tomishige, *Catal. Surv. Asia* **2011**, *15*, 111 – 116; b) Y. Nakagawa, K. Tomishige, *Catal. Today* **2012**, *195*, 136 – 143; c) Y. Nakagawa, M. Tamura, K. Tomishige, *ACS Catal.* **2013**, *3*, 2655 – 2668; d) K. Tomishige, M. Tamura, Y. Nakagawa, *Chem. Rec.* **2014**, *14*, 1041 – 1054; e) Y. Nakagawa, M. Tamura, K. Tomishige, *Catal. Surv. Asia* **2015**, *19*, 249 – 256.
[3] Y. Nakagawa, H. Nakazawa, H. Watanabe, K. Tomishige, *ChemCatChem* **2012**, *4*, 1791 – 1797.
[4] a) S. Koso, I. Furikado, A. Shimao, T. Miyazawa, K. Kunimori, K. Tomishige, *Chem. Commun.* **2009**, 2035 – 2037; b) S. Koso, N. Ueda, Y. Shinmi, K. Okumura, T. Kizuka, K. Tomishige, *J. Catal.* **2009**, *267*, 89 – 92; c) S. Koso, Y. Nakagawa, K. Tomishige, *J. Catal.* **2011**, *280*, 221 – 229; d) M. Chia, Y. J. Pagan-Torres, D. Hibbitts, Q. Tan, H. N. Pham, A. K. Datye, M. Neurock, R. J. Davis, J. A. Dumesic, *J. Am. Chem. Soc.* **2011**, *133*, 12675 – 12689; e) K. Chen, K. Mori, H. Watanabe, Y. Nakagawa, K. Tomishige, *J. Catal.* **2012**, *294*, 171 – 183; f) S. Koso, H. Watanabe, K. Okumura, Y. Nakagawa, K. Tomishige, *Appl. Catal. B* **2012**, *111*, 27 – 37; g) Y. Nakagawa, K. Mori, K. Chen, Y. Amada, M. Tamura, K. Tomishige, *Appl. Catal. A* **2013**, *468*, 418 – 425; h) S. Liu, Y. Amada, M. Tamura, Y. Nakagawa, K. Tomishige, *Catal. Sci. Technol.* **2014**, *4*, 2535 – 2549; i) S. Liu, Y. Amada, M. Tamura, Y. Nakagawa, K. Tomishige, *Green Chem.* **2014**, *16*, 617 – 626; j) B. Pholjaroen, N. Li, Y. Huang, L. Li, A. Wang, T. Zhang, *Catal. Today* **2015**, *245*, 93 – 99.
[5] a) L. Schniepp, H. Geller, *J. Am. Chem. Soc.* **1946**, *68*, 1646 – 1648; b) C. L. Wilson, *J. Am. Chem. Soc.* **1947**, *69*, 3004 – 3006; c) S. Sato, J. Igarashi, Y. Yamada, *Appl. Catal. A* **2013**, *453*, 213 – 218.
[6] a) H. P. Thomas, C. L. Wilson, *J. Am. Chem. Soc.* **1951**, *73*, 4803 – 4805; b) S. Sato, R. Takahashi, N. Yamamoto, E. Kaneko, H. Inoue, *Appl. Catal. A* **2008**, *334*, 84 – 91.
[7] a) K. Chen, S. Koso, T. Kubota, Y. Nakagawa, K. Tomishige, *ChemCatChem* **2010**, *2*, 547 – 555; b) T. Buntara, S. Noel, P. H. Phua, I. Melián-Cabrera, J. G. de Vries, H. J. Heeres, *Angew. Chem. Int. Ed.* **2011**, *50*, 7083 – 7087; *Angew. Chem.* **2011**, *123*, 7221 – 7225; c) T. Buntara, I. Melián-Cabrera, Q. Tan, J. L. Fierro, M. Neurock, J. G. de Vries, H. J. Heeres, *Catal. Today* **2013**, *210*, 106 – 116; d) A. C. Alba-Rubio, C. Sener, S. H. Hakim, T. M. Gostanian, J. A. Dumesic, *ChemCatChem* **2015**, *7*, 3881 – 3886.
[8] A. Yamaguchi, N. Hiyoshi, O. Sato, K. K. Bando, M. Shirai, *Green Chem.* **2009**, *11*, 48 – 52.
[9] O. Agrawal, *Organic chemistry reactions and reagents, Vol. 627*, Goel publishing house, New Delhi, India, **2008**, pp. 686 – 687.
[10] J. Falbe, *Carbon monoxide in organic synthesis, Vol. 10*, Springer Science & Business Media, **2013**, pp. 113 – 118.
[11] a) Q. Zhang, T. Jiang, B. Li, T. Wang, X. Zhang, Q. Zhang, L. Ma, *ChemCatChem* **2012**, *4*, 1084 – 1087; b) J. Zhang, H. Asakura, J. van Rijn, J. Yang, P. Duchesne, B. Zhang, X. Chen, P. Zhang, M. Saeys, N. Yan, *Green Chem.* **2014**, *16*, 2432 – 2437; c) W. Song, Y. Liu, E. Baráth, C. Zhao, J. A. Lercher, *Green Chem.* **2015**, *17*, 1204 – 1218.
[12] J. Lee, Y. Xu, G. W. Huber, *Appl. Catal. B* **2013**, *140*, 98 – 107.
[13] S. Sitthisa, D. E. Resasco, *Catal. Lett.* **2011**, *141*, 784 – 791.
[14] Z. Li, R. S. Assary, A. C. Atesin, L. A. Curtiss, T. J. Marks, *J. Am. Chem. Soc.* **2014**, *136*, 104 – 107.
[15] R. Alamillo, M. Tucker, M. Chia, Y. Pagán-Torres, J. Dumesic, *Green Chem.* **2012**, *14*, 1413 – 1419.
[16] K. Chandler, F. Deng, A. K. Dillow, C. L. Liotta, C. A. Eckert, *Ind. Eng. Chem. Res.* **1997**, *36*, 5175 – 5179.
[17] a) J. He, C. Zhao, D. Mei, J. A. Lercher, *J. Catal.* **2014**, *309*, 280 – 290; b) J. He, L. Lu, C. Zhao, D. Mei, J. A. Lercher, *J. Catal.* **2014**, *311*, 41 – 51.
[18] C. Zhao, Y. Yu, A. Jentys, J. A. Lercher, *Appl. Catal. B* **2013**, *132*, 282 – 292.
[19] D. Andrus, J. R. Johnson, *Org. Synth.* **1943**, 90 – 90.
[20] I. Sádaba, M. L. Granados, A. Riisager, E. Taarning, *Green Chem.* **2015**, *17*, 4133 – 4145.

Manuscript received: December 28, 2016
Revised: January 30, 2017
Accepted Article published: February 10, 2017
Final Article published: ■■ ▮▮, 0000

E. Soghrati, C. Choong, C. K. Poh, S. Kawi, A. Borgna**

■■ – ■■

Single-Pot Conversion of Tetrahydrofurfuryl Alcohol into Tetrahydropyran over a Ni/HZSM-5 Catalyst under Aqueous-Phase Conditions

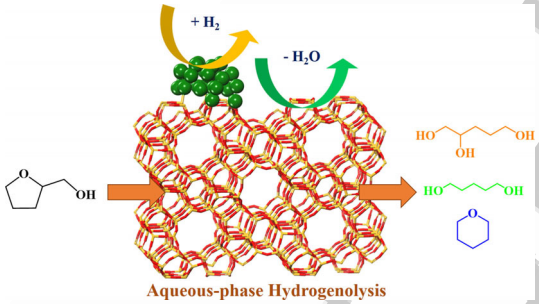

A highly efficient earth-abundant and low-cost Ni/HZSM-5 catalyst was developed for upgrading biomass-derived cyclic ether compounds into valuable chemicals. New reaction products and reaction mechanisms were identified over the catalyst under aqueous-phase conditions, which can contribute to elucidate pathways during the ring-opening reaction.

Converting tetrahydro #furfuryl alcohol into tetrahydropyran by aqueous phase Ni/ #HZSM-5 #catalysis
SPACE RESERVED FOR IMAGE AND LINK

Share your work on social media! *ChemCatChem* has added Twitter as a means to promote your article. Twitter is an online microblogging service that enables its users to send and read text-based messages of up to 140 characters, known as "tweets". Please check the pre-written tweet in the galley proofs for accuracy. Should you or your institute have a Twitter account, please let us know the appropriate username (i.e., @accountname), and we will do our best to include this information in the tweet. This tweet will be posted to the journal's Twitter account @ChemCatChem (follow us!) upon online publication of your article, and we recommended you to repost ("retweet") it to alert other researchers about your publication.

Please check that the ORCID identifiers listed below are correct. We encourage all authors to provide an ORCID identifier for each coauthor. ORCID is a registry that provides researchers with a unique digital identifier. Some funding agencies recommend or even require the inclusion of ORCID IDs in all published articles, and authors should consult their funding agency guidelines for details. Registration is easy and free; for further information, see http://orcid.org/.

Elmira Soghrati
Catherine Choong
Chee Kok Poh
Sibudjing Kawi
Armando Borgna